Chemical Engineering Communications

ISSN: 0098-6445 (Print) 1563-5201 (Online) Journal homepage: https://www.tandfonline.com/loi/gcec20

Facile Synthesis of the Novel Ag[1-butyl 3-methyl imidazolium]Br Nanospheres for Efficient Photodisinfection of Wastewaters

Mohsen Padervand

To cite this article: Mohsen Padervand (2016) Facile Synthesis of the Novel Ag[1-butyl 3-methyl imidazolium]Br Nanospheres for Efficient Photodisinfection of Wastewaters, Chemical Engineering Communications, 203:11, 1532-1537, DOI: 10.1080/00986445.2016.1215982

To link to this article: https://doi.org/10.1080/00986445.2016.1215982

Chemical Engineering Communications, 203:1532–1537, 2016
Published with license by Taylor & Francis Group, LLC
ISSN: 0098-6445 print/1563-5201 online
DOI: 10.1080/00986445.2016.1215982

Facile Synthesis of the Novel Ag[1-butyl 3-methyl imidazolium]Br Nanospheres for Efficient Photodisinfection of Wastewaters

MOHSEN PADERVAND

Department of Chemistry, University of Maragheh, Maragheh, Iran

Ag[1-butyl 3-methyl imidazolium]Br nanospheres were prepared by a coprecipitation method at ambient temperature. The products were characterized by X-ray diffraction (XRD), scanning electron microscopy (SEM), transmission electron microscopy (TEM), diffusion reflectance spectra (DRS), the Brunauer–Emmett–Teller (BET) nitrogen adsorption–desorption isotherms, and Fourier transform infrared spectroscopy (FT-IR) analysis methods. The photocatalytic properties were evaluated by degradation of acid blue 92 (AB92) and rhodamine B (RB) dye solutions under visible light and the obtained results were discussed. According to the recycling experiments, the samples could efficiently decrease the concentration of the pollutant after four times of repeated using. To assure the practical capacity, photodegradation of a real wastewater produced in the textile industry was studied under the same conditions and the results indicated that the absorption in all wavelengths reduced impressively by the photocatalytic treatment. Furthermore, the antimicrobrial activity was investigated by photoinactivation of S. aureus bacteria in the visible light and the results implied that the prepared samples were able to prevent the growth of bacteria colonies after the reaction time.

Keywords: Bacteria; Ionic liquid; Nanosphere; Photodegradation; Wastewater

Introduction

To develop the practical applications of visible-light photoactive structures in facing the increasingly serious environmental problems, silver-based nano-micro materials have received much attention because of their promising activity under solar energy. To address this issue, various silver halide-based structures (Wang et al., 2010; An et al., 2010; Wang et al., 2012a, 2012b, 2012d; Xie et al., 2015), silver orthophosphates (Yi et al., 2010; Wang et al., 2012c), silver chromates (Ouyang et al., 2008), and silver vanadates (Li et al., 2007) have been widely studied. Because of their intriguing electronic, electromechanical, optoelectronic, and photocatalytic properties, silver halide-included systems have attracted many researchers attention. Among them, Ag-AgX (X=Cl, Br, I) nanostructures have been proved to be promising plasmonic photocatalysts (Azimzadehirani et al., 2011; Elahifard et al., 2007; Esmaeili and Entezari, 2016). The metallic Ag^{o} nanoparticles bonded to the structures could considerably affect the electronic structures and suppress the corrosion of the silver halides under illumination (Zhao et al., 2012; Wang et al., 2008). Many attempts have been made to improve the photocatalytic performance of the large-band gap semiconductors via coupling with silver halides (Cheng et al., 2011; Wang et al., 2012e).

Owing to many interesting properties such as good electric conductivities, negligible vapor pressures, good thermal stabilities, wide liquid temperature ranges and electrochemical windows, and high solvation interactions with both polar and non-polar compounds, ionic liquids (ILs) have been vastly considered in the synthesis of new nanosystems with a wide range of industrial usages (Plechkova and Seddon, 2008). In addition, a variety of high-quality photosensitive nanomaterials with controllable special morphology and improved photocatalytic properties have been prepared by using of ILs as complexing agents (An et al., 2010; Chen et al., 2015; He et al., 2007; Xia et al., 2016).

Herein, we reported a facile one-step synthesis method to fabricate the Ag[BMIM]Br nanospheres using 1-Butyl-3-methylimidazolium bromide([BMIM]Br) IL and silver nitrate salt as the Br and Ag resource, respectively. The prepared nanostructures were used for the degradation of AB92 and RB dye solutions and S. aureus bacteria under visible

Address correspondence to Dr. Mohsen Padervand, Faculty of Science, Department of Chemistry, University of Maragheh, Maragheh 55181-83111, Tabriz, Iran. E-mail: padervand@maragheh.ac.ir

Color versions of one or more of the figures in the article can be found online at www.tandfonline.com/gcec.

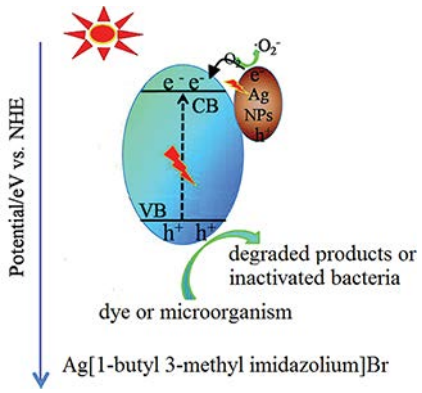

Sch. 1. Photocatalytic degradation of dye compounds and bacteria over the products.

illumination. The photocatalytic process is schematically shown in Scheme 1.

Experimental

The synthesis was simple and fast which involved the mixing of two precursor solutions as follows: first, an aqueous solution (50 mL) contained 5 g of urea and 0.1 mL of the IL, and the second contained 1.07 g of $AgNO_3$ in 30 mL of double distilled water. The mixture was stirred at room temperature for 45 min. The products were filtered, washed repeatedly with ethanol and distilled water, and dried at 60°C overnight.

The photocatalytic tests were performed in a reactor surrounded by a circulating water jacket to maintain the constant temperature. A 125 W mercury lamp (MBF-OSRAM) with UV cut-off filter was used as the irradiation source. The absorption of the dyes was determined by UV–vis spectrophotometer (GBC Cintra40) at $\lambda = 574$ and 552 nm, which are the λ_{max} values of AB92 and RB solutions, respectively. The antibacterial experiments were performed under the operational conditions which were explained elsewhere (Padervand et al., 2012; Padervand et al., 2013).

Results and Discussion

Optical absorption of the nanospheres was studied by UV–vis spectra. As indicated in Figure 1a, the measured pattern for the Ag[BMIM]Br nanospheres shows an obvious absorption in the visible region at wavelength larger than 700 nm. According to the equation $E_g = 1239.8/\lambda$ (Hu et al., 2009), the band gap, E_g, of the photocatalyst was estimated to be less than 1.77 eV, which describes the high tendency of as-prepared nanospheres to absorb the low-energy photons. Findings from studying the morphology regularity and photoactivity of the AgBr nanostructures demonstrated that the band gap was dramatically shifted to the higher wavelengths when the morphology and crystal shape were regular (Li et al., 2013). In the present method which is more time-consuming, we prepared the regular products without using any additional agents such as polymeric compounds.

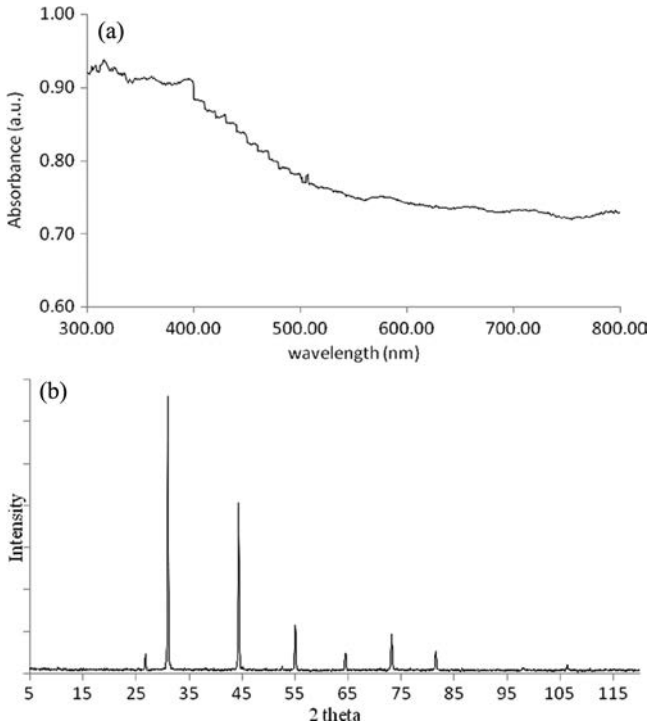

Fig. 1. (a) The UV–vis spectrum and (b) XRD pattern of the prepared nanospheres.

In addition, the band gap shifted impressively to the low energy level. From Figure 1b, which exhibits the X-ray diffraction (XRD) pattern of the prepared photocatalyst, the products involve the face-centered cubic structure of AgBr (JCPDS no. 6–438) and a small amount of Ag. Peaks with 2Θ values of 26.7, 31.0, 44.3, and 55.0 are attributed to (111), (200), (220), and (222) crystal planes of the cubic silver bromide. The observable peak at $2\Theta = 65.0°$ is assigned to the Ag^0 crystals in the structures (JCPDS no. 04–0783). From Figure 2a, which shows the results of the Fourier transform infrared spectroscopy (FT-IR) analysis, the obvious bands at 1465 and 1655 cm^{-1} are assigned to the C=C and C=N stretching vibrations. The other ones at 2941 and 2877 cm^{-1} are attributed to the aliphatic symmetric and asymmetric C−H stretching vibrations of butyl chain and methyl attached to the imidazolium ring. Furthermore, one can find the characteristic peaks of C−N stretching vibrations at 748.3 and 623 cm^{-1} (Cha et al., 2014). The broaden peak at higher than 3400 cm^{-1} is due to H_2O molecules adsorbed on the surface of the sample. The results of Brunauer−Emmett−Teller (BET) analysis show that the specific surface area of the nanospheres was 17.5 $m^2\ g^{-1}$. The obtained hysteresis loop from the N_2 adsorption–desorption measurement (Figure 2b) demonstrated the porosity of the nanospheres. Moreover, Barrett-Joyner-Halenda (BJH) analysis was performed to find the pore size distribution and the obtained results indicated that the pores size is concentrated between 2 and 10 nm (Figure 2c). Morphological studies were performed by using of scanning electron microscopy (SEM) and transmission electron

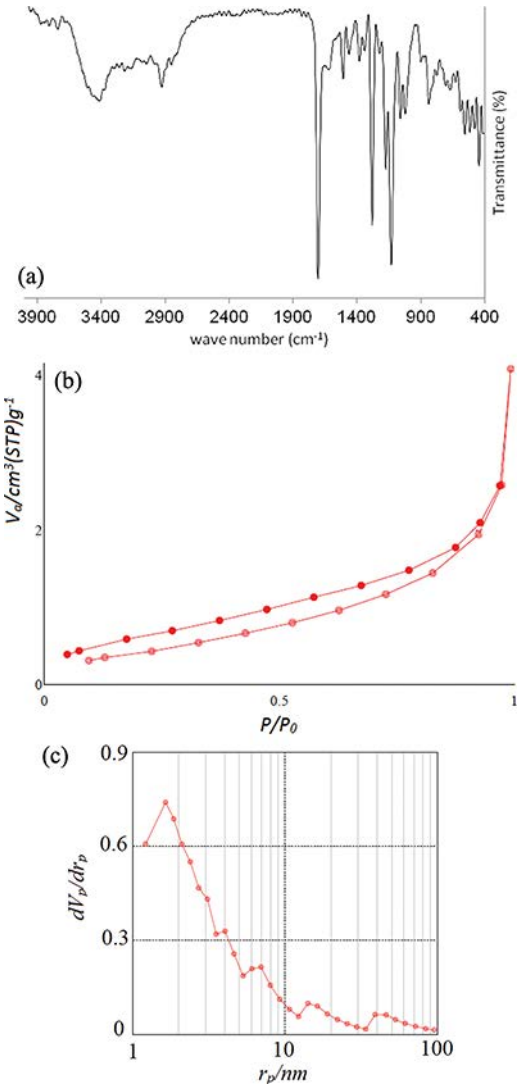

Fig. 2. (a) FT-IR spectrum and (b) nitrogen adsorption–desorption isotherm of Ag[BMIM]Br nanospheres.

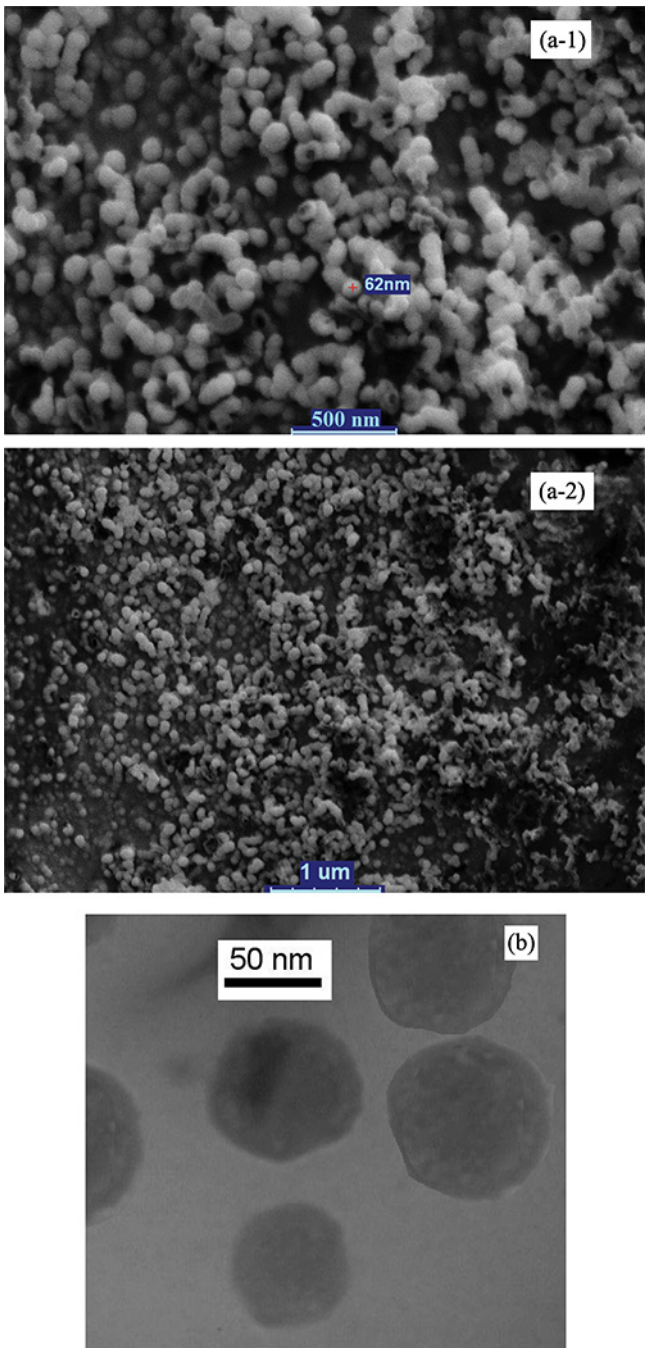

Fig. 3. SEM micrographs (a-1 and a-2) and TEM images (b) of the nanospheres.

microscopy (TEM) images. From the SEM images, the nanostructures exhibit uniform size and regular morphology and the average size is ~60 nm. In order to further examination of the structural morphology, TEM analysis was performed and the results (Figure 3b) confirmed that the products have spherical shape. From Figure 3b, the average particle size is similar to that of determined by the SEM micrographs. The photocatalytic properties of our products are firstly evaluated by photodegradation of AB92 and RB dyes under visible light and the results are displayed in Figure 4a. As shown in Figure 4a, the removal efficiency is promising over the nanospheres and the fastest reaction was related to the degradation of AB92 solution. Besides, the result of photodegradation of the dual dye solution (AB92+RB, 10 ppm respect to each dye) showed that the AB92 concentration decreased much faster than RBs. This can be explained by considering the chromophoric structure of the compounds. From the chemical structures of the compounds (Figure 4b), the chromophoric group of RB, a cationic dye, could resonant between the two sides of the structure. Meanwhile, this is not possible for that of AB92 which is an anionic dye. Due to the mentioned reasons the degradation process was determined to be much slower for the former case. The surface of the photocatalyst is partly positive because of the $[BMIM]^+$ components in the structures which increases the sorption capacity toward the anionic compounds in the solution. As a reasonable expectation, AB92 dye would be adsorbed on the surface more

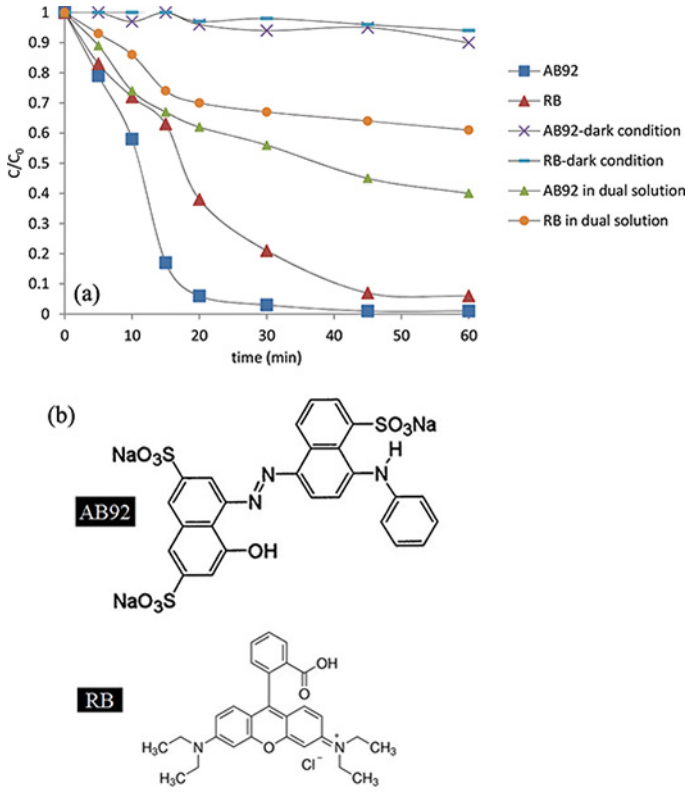

Fig. 4. (a) Photodegradation of RB and AB92 over the prepared nanospheres under visible light (dye concentration-volume: 20 ppm-50 mL, catalyst amount: 0.02 g, temperature: 27°C, pH: 6.8). (b) Chemical structures of AB92 and RB.

efficient than RB during the photocatalytic process and under the dark. All the above statements demonstrate that the prepared nanospheres are very suitable for decomposition of the anionic organic pollutants rather than the cationic ones. As an important issue in the practical applications, the stability of the photocatalyst was evaluated by the cycling experiments. As shown in Figure 5, the Ag[BMIM]Br

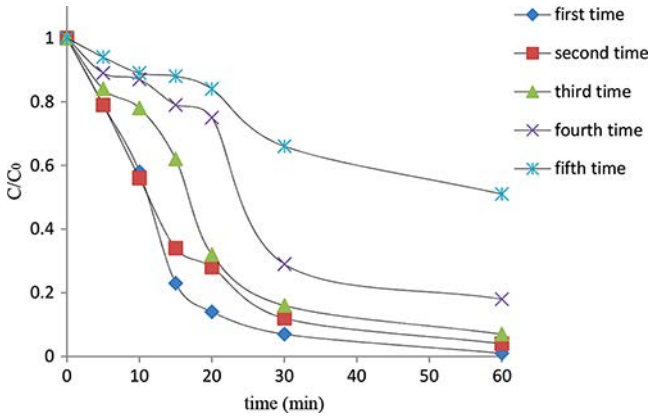

Fig. 5. The result of recycling experiments over the prepared photocatalyst (dye (AB92) concentration-volume: 20 ppm-50 mL, catalyst amount: 0.02 g, temperature: 27°C, pH: 6.8).

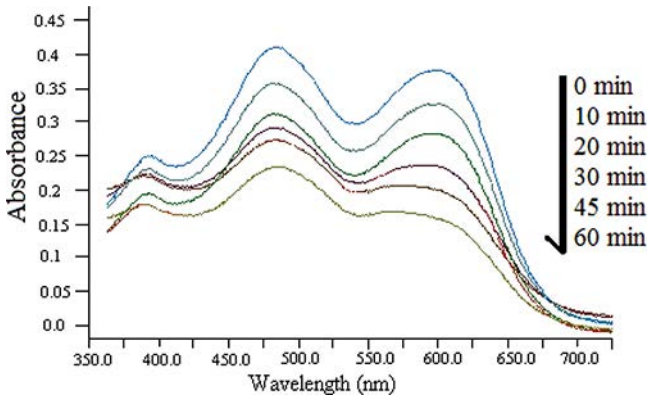

Fig. 6. Photocatalytic degradation of the real waste water provided from the textile industry (catalyst amount: 0.02 g, temperature: 27°C, pH: 6.8).

nanospheres were almost stable after 5 times of subsequent using and the activity decreased gently. The rate constants for these curves which followed the first-order kinetics were calculated to be: 0.231, 0.205, 0.180, 0.135, and 0.078 s^{-1}, respectively. According to the reports, surface photocorrision of the silver-based catalysts is the most important factor that influences their activity under irradiation (Yi et al., 2010; Wang et al., 2012; Ouyang et al., 2008; Li et al., 2007). About the current samples, the [BMIM] component acts as a tightening linkage and delays the disruption of the silver bromide structures during the light absorption. As a typical practical application, the ability of as-prepared nanospheres for the decomposition of a real wastewater sample from the textile industries was evaluated under the same experimental conditions. As seen in Figure 6, the total con-

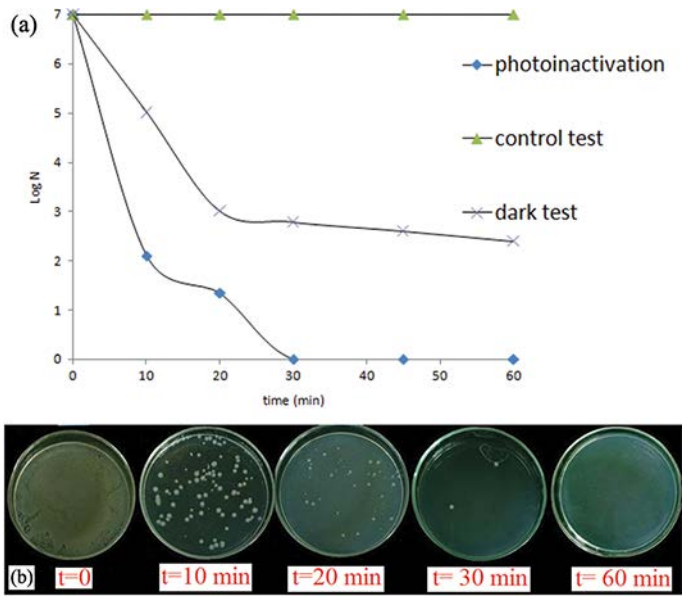

Fig. 7. (a) The results of the antibacterial tests over the products. (b) The number of the bacteria remained after the photocatalytic treatment times.

centration in all the wavelengths decreased by time and the photocatalyst is able to remove the wastewater under solar light very well.

As an extra examination, photoinactivation of S. aureus, a gram positive bacterium, in visible light was investigated over the products. As shown in Figure 7, almost all the bacteria were killed under the photocatalytic conditions in 30 min indicating highly antibacterial capacity of the nanospheres. According to the earlier reports, antimicrobial mechanism is related to the formation of free radicals like $OH^{\bullet}$, $O_2^{\bullet-}$, and $HO_2^{\bullet}$ on the surface of the illuminated photocatalyst (Chung et al., 2009). Furthermore, the time evolution of the bacteria in the presence of the nanostructures in dark indicated that the number of the bacteria slightly decreased. We propose that the electrostatic interactions between the surface of the nanostructures contained cationic [BMIM] ingredients and the cell wall of the gram positive bacteria, which includes different anionic polymers such as phospholipids and peptidoglycans, block the vital pores of the membrane and disrupt the microorganism life cycle. This results in the inactivation of the bacteria and preventing the replication process.

Conclusions

In summary, we reported the one-step synthesis of the novel photoresponsive Ag[BMIM]Br nanospheres using a water soluble IL as the Br resource. The prepared samples were well-dispersed and easy to separate from the reaction medium. The nanospheres showed an excellent photocatalytic performance for the degradation of RB and AB92 dyes under visible illumination. The results of the recycling experiments approved the stability of the products after four times of repeated using. As a typical industrial application, photodegradation of a real wastewater sample over the products was investigated and according to the obtained results, the nanostructures were able to remove the pollution from the medium, effectively. The results for the inactivation of the gram positive bacterial cells in visible light exhibited that the products had incredible antimicrobial activity. The antibacterial activity at dark was assigned to the electrostatic interactions between the positive surfaces of the products and the anionic polymers which are the major constituents of the bacterial cell wall.

References

An, C., Peng, S., and Sun, Y. (2010). Facile synthesis of sunlight-driven AgCl:Ag plasmonic nanophotocatalyst, *Adv. Mater.*, **22**, 2570–2574.

Azimzadehirani, M., Elahifard, M. R., Haghighi, S., and Gholami, M. R. (2011). Highly efficient hydroxyapatite/TiO_2 composites covered by silver halides as E. coli disinfectant under visible light and dark media, *Photochem. Photobiol. Sci.*, **12**, 1787–1794.

Cha, S., Ao, M., Sung, W., Moon, B., Ahlstrom, B., Johansson, P., Ouchi, Y., and Kim, D. (2014). Structures of ionic liquid-water mixtures investigated by IR and NMR spectroscopy, *Phys. Chem. Chem. Phys.*, **28**, 9591–601.

Chen, D., Wang, Z., Du, Y., Yang, G., Ren, T., and Ding, H. (2015). In situ ionic-liquid-assisted synthesis of plasmonic photocatalyst Ag/AgBr/g-C_3N_4 with enhanced visible-light photocatalytic activity, *Catal. Today*, **258**, 41–48.

Cheng, H. F., Huang, B. B., Wang, P., Wang, Z. Y., Lou, Z. Z., and Wang, J. P. (2011). In situ ion exchange synthesis of the novel Ag/AgBr/BiOBr hybrid with highly efficient decontamination of pollutants, *Chem. Commun.*, **47**, 7054–7056.

Chung, C. J., Lin, H. I., Chou, C. M., Hsieh, P. Y., Hsiao, C. H., Shi, Z. Y., and He, J. L. (2009). Inactivation of Staphylococcus aureus and Escherichia coli under various light sources on photocatalytic titanium dioxide thin film, *Surf. Coat. Tech.*, **203**, 1081–1085.

Elahifard, M. R., Rahim-Nejad, S., Haghighi, S., and Gholami, M. R. (2007). Apatite-coated Ag/AgBr/TiO_2 visible-light photocatalyst for destruction of bacteria, *J. Am. Chem. Soc.*, **129**, 9552–9553.

Esmaeili, A., and Entezari, M. H. (2016). Sonosynthesis of an Ag/AgBr/Graphene-oxide nanocomposite as a solar photocatalyst for efficient degradation of methyl orange, *J. Colloid Interface Sci.*, **15**, 227–237.

He, Y., Li, D., Chen, Z., Chen, Y., and Fu, X. (2007). New synthesis of single-crystalline $InVO_4$ nanorods using an ionic liquid, *J. Am. Ceram. Soc.*, **90**, 3698–3703.

Hu, W. B., Li, L. P., Li, G. S., Tang, C. L., and Sun, L. (2009). High-quality brookite TiO_2 flowers: synthesis, characterization, and dielectric performance, *Cryst. Growth Des.*, **9**, 3676–3682.

Li, B., Wang, H., Zhang, B., Hu, P., Chen, C., and Guo, L. (2013). Facile synthesis of one dimensional AgBr@Ag nanostructures and their visible light photocatalytic properties, *ACS Appl. Mater. Inter.*, **5**, 12283–12287.

Li, D., Duan, X., Qin, Q., Fan, H., and Zheng, W. (2007). Facile synthesis of novel α-Ag_3VO_4 nanostructures with enhanced photocatalytic activity, *Cryst. Eng. Comm.*, **15**, 8933–8936.

Ouyang, S., Li, Z. S., Ouyang, Z., Yu, T., Ye, J. H., and Zou, Z. G. (2008). Correlation of crystal structures, electronic structures, and photocatalytic properties in a series of Ag-based oxides: $AgAlO_2$, $AgCrO_2$, and Ag_2CrO_4, *J. Phys. Chem. C*, **112**, 3134–3141.

Padervand, M., Elahifard, M. R., Vatan-Meidanshahi, R., Ghasemi, S., Haghighi, S., and Gholami, M. R. (2012). Investigation of the antibacterial and photocatalytic properties of the zeolitic nanosized AgBr/TiO_2 composites, *Mat. Sci. Semicon. Proc.*, **15**, 73–79.

Padervand, M., Salari, H., Sadeghzadeh Darabi, F., and Gholami, M. R. (2013). Kinetic and mechanistic study of p-nitrochlorobenzene photoreduction and Bacillus inactivation over aluminosilicate-based nanocomposites, *Monatsh. Chem.*, **144**, 589–596.

Plechkova, N. V., and Seddon, K. R. (2008). Applications of ionic liquids in the chemical industry, *Chem. Soc. Rev.*, **37**, 123–150.

Wang, D. S., Duan, Y. D., Luo, Q. Z., Li, X. Y., An, J., and Bao, L. L. (2012a). Novel preparation method for a new visible light photocatalyst: mesoporous TiO_2 supported Ag/AgBr, *J. Mater. Chem.*, **22**, 4847–4854.

Wang, H., Gao, J., Guo, T. Q., Wang, R. M., Guo, L., Liu, Y., and Li, J. H. (2012b). Facile synthesis of AgBr nanoplates with exposed {111} facets and enhanced photocatalytic properties, *Chem. Commun.*, **48**, 275–277.

Wang, H., He, L., Wang, L. H., Hu, P. F., and Guo, L. (2012c). Facile synthesis of Ag_3PO_4 tetrapod microcrystals with an increased percentage of exposed {110} facets and highly efficient photocatalytic properties, *Cryst. Eng. Comm.*, **14**, 8342–8344.

Wang, H., Li, Y., Li, C., He, L., and Guo, L. (2012d). Facile synthesis of AgBr nanocubes for highly efficient visible light photocatalysts, *Cryst. Eng. Comm.*, **14**, 7563–7566.

Wang, H., Yang, J. T., Li, X. L., Zhang, H. Z., Li, J. H., and Guo, L. (2012e). Facet-dependent photocatalytic properties of AgBr nanocrystals, *Small*, **8**, 2802–2806.

Wang, P., Huang, B. B., Zhang, X. Y., Qin, X. Y., Dai, Y., and Wei, J. Y. (2008). Ag@AgCl: A highly efficient and stable

photocatalyst active under visible light, *Angew. Chem. Int. Edit.*, **47**, 7931–7933.

Wang, P., Huang, B., Zang, Q., Zang, X., Qin, X., Dai, Y., Zang, J., Yu, J., Liu, H., and Lou, Z. (2010). Highly efficient visible light plasmonic photocatalyst Ag@Ag(Br, I), *Chem. Eur. J.*, **16**, 10042–10047.

Xia, J., Ji, M., Li, W., Di, J., Xu, H., He, M., Zhang, Q., and Li, H. (2016). Synthesis of erbium ions doped BiOBr via a reactive ionic liquid with improved photocatalytic activity, *Colloid Surface A*, **489**, 343–350.

Xie, R., Zhang, L., Xu, H., Zhong, Y., Sui, X., and Mao, Z. (2015). Fabrication of Z-scheme photocatalyst Ag–AgBr@$Bi_{20}TiO_{32}$ and its visible-light photocatalytic activity for the degradation of isoproturon herbicide, Fabrication of Z-scheme photocatalyst Ag–AgBr@Bi_{20} TiO_{32} and its visible-light photocatalytic activity for the degradation of isoproturon herbicide, *J. Mol. Catal. A: Chem.*, **406**, 194–203.

Yi, Z., Ye, J., Kikugawa, N., Kako, T., Quyang, S., Williams, H. S., Yang, H., Cao, J., Luo, W., Liu, Y., and Withers, R. L. (2010). An orthophosphate semiconductor with photooxidation properties under visible-light irradiation, *Nat. Mater.*, **9**, 559–564.

Zhao, Y. Y., Kuai, L., Geng, B. Y. (2012). Low-cost and highly efficient composite visible light-driven Ag–AgBr/γ-Al_2O_3 plasmonic photocatalyst for degrading organic pollutants, *Catal. Sci. Technol.*, **2**, 1269–1274.